Talbot Effect On The 2-Sphere

IGL Scholars: Haotian Ju, Jiazheng Wang, Yiheng Zhou, Graduate Mentor: Ryan McConnell, Faculty Mentor: Burak Erdoğan

Introduction

Dispersion is a characteristic feature of certain types of partial differential equations, and the behavior of their solution profiles can vary significantly depending on the algebraic properties of time. In particular, when considering square wave initial data and time that is a rational multiple of the period, the solution takes on a piecewise step-like form.

However, when time is an irrational multiple of the period, the solution becomes a continuous but non-differentiable fractal curve. This striking phenomenon is commonly referred to as the "Talbot Effect" and is characterized by the existence of two distinct types of solution behavior for dispersive PDEs, depending on the choice of time.

There is currently limited understanding of how the "Talbot Effect" manifests itself on $\mathbb{S}^2$. As such, our primary objective in this research is to use numerical methods to investigate the behavior of the "Talbot Effect" on the 2-Sphere.

Backgrounds and Methods

Basic model: linear Schrödinger

$$\begin{cases} iu_t + \triangle_{\mathbb{S}^2} = 0 \\ u(x,0) = g(x), \end{cases}$$

where u is a function $\mathbb{S}^2 \to \mathbb{C}$, and $g(x) : \mathbb{S}^2 \to \mathbb{R}$ is some *real valued initial data.*

Starting with Fourier Series on $\mathbb{S}^2$:

$$g(x) = \sum_{n=0}^{\infty} \sum_{k=-n}^{n} a_{n,k} Y^{n,k}(x), \quad a_{n,k} = \int_0^{\pi} \int_0^{2\pi} g(\theta,\varphi) Y^{n,k}(\theta,\varphi) \sin(\theta)\, d\varphi d\theta,$$

we find that the solution is of the form:

$$u(\phi,\theta,t) = \sum_{n=0}^{\infty} \sum_{k=-n}^{n} a_{n,k} e^{in(n+1)} Y^{n,k}.$$

We may choose the $Y^{n,k}$ to be real so that the real part of the solution should be:

$$\Re(u(\phi,\theta,t)) = \sum_{n=0}^{\infty} \sum_{k=-n}^{n} a_{n,k} \cos(tn(n+1)) Y^{n,k},$$

which will enable us to visualize this for different t values.

We can see the real solutions in 3-dimensional plots:

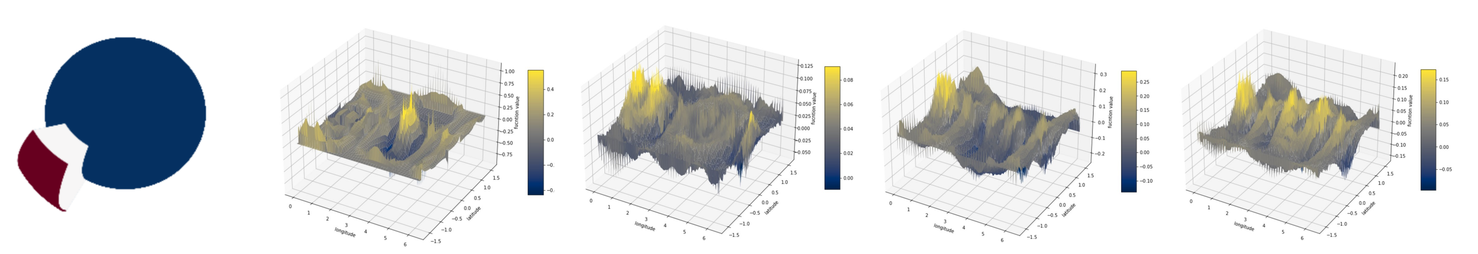

Left to right: initial data, $\Re u$ for $t = \pi/10$, $\Re u$ for $t = \pi^2/100$, $\Re u$ for $t = \sqrt{2}\pi/10$, $\Re u$ for $t = e\pi/10$

We also change the initial data and perform the above with triangular data.

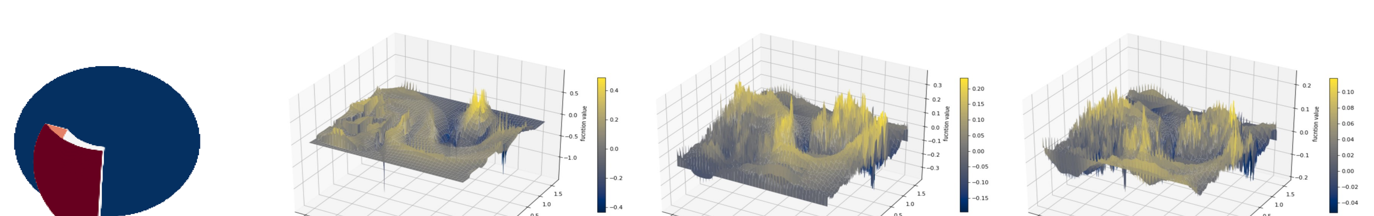

Left to right: new initial data, $\Re u$ for $t = \pi/10$, $\Re u$ for $t = \pi^2/10$, $\Re u$ for $t = e\pi/10$

Definition (Box-Counting Dimension): The Dimension of a bounded set E is given by

$$\overline{\dim}\mathrm{E} = \lim_{\epsilon \to 0} \frac{\log(N(\epsilon))}{\log \frac{1}{\epsilon}},$$

where $N(\epsilon)$ is the minimum number of $\epsilon-$boxes required to cover E.

We use the smallest number of boxes to cover the whole surface, where the boxes have length ϵ. To approximate this process, we split $\mathbb{S}^2$ into squares of side length ϵ. Above each box, we calculate the maximum of the function and the minimum of the function and divide this number by ϵ. This tells us approximately how many boxes are required to cover the graph above the square, and summing over each square tells us how many are required to cover the entire graph. We can constantly improve our results by increasing the resolution–the more boxes we have, the better our results will be.

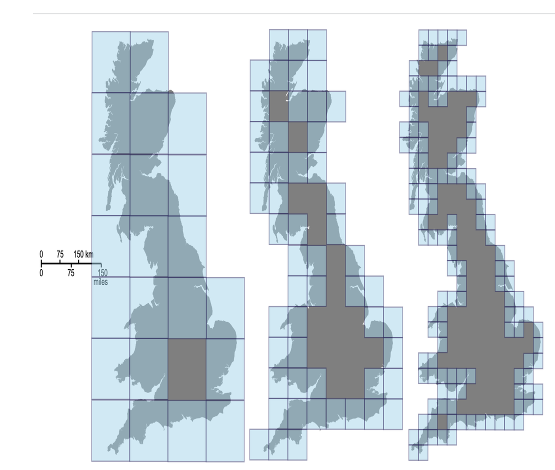

Example of the process of calculating the box dimension of the coastline of Great Britain.

Using a sequence of decreasing ϵ's we calculating $\log N(\epsilon)$ and $\log(1/\epsilon)$. Below are two methods we use.

Linear Regression Method

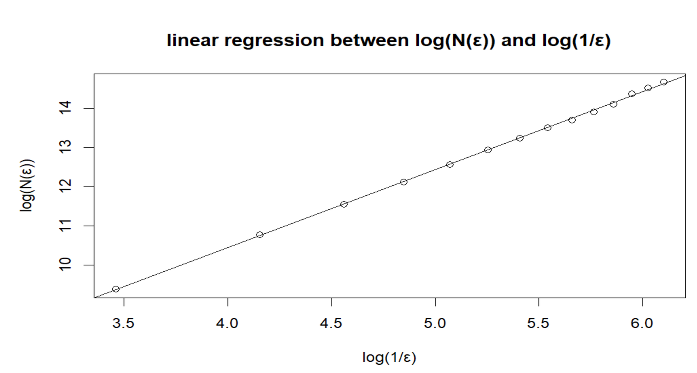

Using a sequence of decreasing ϵ's we regress $\log N(\epsilon)$ and $\log(1/\epsilon)$.This is the graph we got by regressing the initial rectangle data, which has a slope of 2.

Mean Method

For different pairs of

$$(\log(N(\epsilon)), \log\frac{1}{\epsilon})$$

corresponding to different ϵ, we directly calculate the $\frac{\log(N(\epsilon))}{\log\frac{1}{\epsilon}}$ and take the mean.

This slightly speeds up the calculation, and conforms with existing literature.

Results

From the Box-Counting Dimension, although we cannot take $\epsilon \to 0$, we plotted the best-fitting line by using the $(\log(N(\epsilon)), \log\frac{1}{\epsilon})$ with different ϵ values to approximate the dimension for the surface. From the result, we can see that the best-fitting line's slope is 1.99, which is close to 2.

Rectangular data: 2000×4000

When $t = 0$ we find that the fractal dimension is morally 2. This behavior changes dramatically when we consider $t = \pi/10$, in which case we calculate the fractal dimension to be 2.75 (Mean Method). When $t = e\pi/10$ we calculate the fractal dimension to be 2.67 (Mean Method). This doesn't seem to conform to what one would expect based on the picture.

Triangular data: 2000×4000

After testing with the rectangular data, we then tried the triangular initial data. We got 2.2 when $t = 0$. Then we tried $t = \pi/10$ (rational multiple) and got 2.66 (Mean Method). Finally, we experimented at $t = e\pi/10$ (irrational multiple) and got 2.74 (Mean Method) as our result. This result matched our expectations.

However, this result can be improved by choosing more sampling points. We originally chose to run a sampling size of 10000, but then we had problems with the significantly extended run time. Instead, we did 5000 samplings.

Rectangular data: $5000 \times 10,000$

When $t = \pi/10$ (rational multiple), for the linear regression method we get 2.083, and for the mean method, we get 2.733. For $t = e\pi/10$ (irrational multiple) we get 2.2645 (Regression Method), and 2.941 (Mean Method). This matches what we expected according to the picture for the irrational time case.

Triangular data: $5000 \times 10,000$

When $t = \pi/10$ (rational multiple) we get 2.0649 (Regression Method), and 2.8079 (Mean Method). On the other hand, when $t = e\pi/10$ (irrational multiple), we get 2.281(Regression Method), and 2.958 (Mean Method). This also matches what we expected according to the picture for the irrational time case.

Observations from the above data

We observed that graphs for irrational times tend to be more chaotic as there were more spikes around them. Conversely, the graphs for rational times looked smoother. It is reasonable to expect more covering boxes for irrational times as we need to cover all the spikes as well. Our result is closer to the expectation as the number of sample points increases.

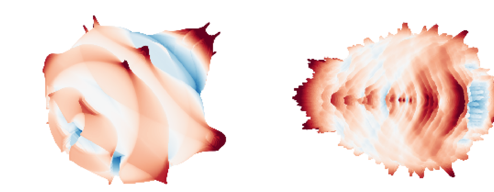

Left to right: Surface plots for $\Re u$ for $t = \pi/10$, $\Re u$ for $t = e\pi/10$

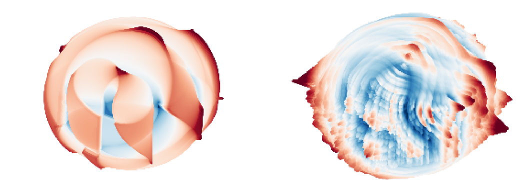

Left to right: Surface plots for $\Re u$ for $t = \pi/10$, $\Re u$ for $t = e\pi/10$ in the new initial data

Future Directions

Above we show approximations to the fractal dimension of solutions to the linear Schrödinger equation on $\mathbb{S}^2$ under different initial conditions at several different times, t, separately. We would like to test for more initial data and see how the solutions change corresponding to new initial data and different t values. So far our initial matrices have only been in the shape of a rectangle and a triangle in the $2\pi \times \pi$ area, but the code developed is capable of handling very general data. We would like to test for random shapes to make our result more generalized.

In the Box-Counting Dimension process, we used an algorithm that may have some limitations that may make the final result somewhat inaccurate, especially related to distortions near the north and south pole. Additionally, because the spherical harmonics $Y^{n,k}$ are not simple objects like e^{inx}, we very quickly run into runtime issues that seriously hamper progress. In our future work, we would like to not only create more accurate algorithms that can reduce the error in counting the number of boxes to cover the surface but also better overcome the distortion issues.

References

[1] Erdogan, M. B., Huynh, C.N.Y., McConnell, R. (2023, April 24). Talbot effect on the sphere and torus for $d > 2$. arXiv.org. Retrieved April 30, 2023, from `https://arxiv.org/abs/2304.12363`

[2] File:great britain box.svg. Wikimedia Commons.(n.d.). Retrieved April 30, 2023, from `https://commons.wikimedia.org/wiki/File:Great_Britain_Box.svg`

[3] SHTools: Tools for working with spherical harmonics.(n.d.). Retrieved May 1, 2023, from `https://agupubs.onlinelibrary.wiley.com/doi/full/10.1029/2018GC00752`

Support for this project was provided by the Illinois Geometry Lab and the Department of Mathematics at the University of Illinois at Urbana-Champaign.